Journal of ELECTRONIC MATERIALS, Vol. 43, No. 11, 2014
DOI: 10.1007/s11664-014-3340-x

Hall Effect Studies of AlGaAs Grown by Liquid-Phase Epitaxy for Tandem Solar Cell Applications

XIN ZHAO,[1,2] KYLE H. MONTGOMERY,[1] and JERRY M. WOODALL[1]

1.—Department of Electrical and Computer Engineering, University of California, Davis, CA 95616, USA. 2.—e-mail: xinzhao@ucdavis.edu

We report results from Hall effect studies on $Al_xGa_{1-x}As$ (x = 0.23–0.24) with bandgap energies of 1.76 ± 0.01 eV grown by liquid-phase epitaxy (LPE). Room-temperature Hall measurements on unintentionally doped AlGaAs revealed p-type background doping for concentrations in the range 3.7–5.2 × 10^{16} cm^{-3}. Sn, Te, Ge, and Zn-doped AlGaAs were also characterized to study the relationship between doping concentrations and the atomic fractions of the dopants in the melt. Temperature-dependent Hall measurements were performed to determine the activation energies of the four dopants. Deep donor levels (DX centers) were dominant for Sn-doped $Al_{0.24}Ga_{0.76}As$, but not for Te-doped $Al_{0.24}Ga_{0.76}As$. Comparison of the temperature-dependent Hall effect results for unintentionally and intentionally doped $Al_{0.24}Ga_{0.76}As$ indicated that the impurity contributing to the p-type background doping had the same activation energy as Mg. We thus suggest a Te-doped emitter and an undoped or Ge-doped base to maximize the efficiency of $Al_xGa_{1-x}As$ ($x \sim 0.23$) solar cells grown by LPE.

Key words: AlGaAs, liquid-phase epitaxy, Hall effect, doping, tandem solar cell

INTRODUCTION

There is increasing interest in seeking top sub-cell materials for dual-junction solar cells based on c-Si bottom sub-cells.[1] Theoretically, a top sub-cell bandgap of ~1.75 eV enables near-optimum power-conversion efficiency of more than 37% under one-sun AM1.5G conditions, assuming an optimized c-Si bottom sub-cell.[2] Lang et al.[3] optimized a metamorphic GaAsP top sub-cell grown on c-Si bottom sub-cells by using graded buffer layers. However, a large number of threading dislocations prevented the open-circuit voltage from reaching its theoretical optimum. AlGaAs is an alternative to GaAsP as a material for the top sub-cell with tunable direct bandgap from 1.42 eV to 2 eV.[4] AlGaAs can be grown lattice-matched on a GaAs substrate, and can then be bonded to a Si bottom sub-cell with the native GaAs substrate subsequently removed.[5] Direct growth of AlGaAs on GaP/Si superstrates is also feasible because efficient electroluminescence has been observed from liquid-phase epitaxy (LPE)-grown AlGaAs on GaP.[6] Growth of Al-rich AlGaAs by use of different techniques, for example molecular beam epitaxy (MBE) or metalorganic chemical vapor deposition (MOCVD), is, however, typically plagued by oxygen incorporation, which reduces the quality of the material.[7] Because LPE is known to be suitable for growing high-purity AlGaAs, because of the liquid–solid growth interface,[8] it is also a promising method for growth of efficient AlGaAs solar cells. It was, therefore, used in this work for our Hall studies of AlGaAs epilayers.

Doping is an essential part of optimization of solar cell performance. For example, too heavy or too light doping of the base will lead to an under-optimized open-circuit voltage because of a large dark saturation current. Moreover, deep donor levels (DX centers) have recently been shown to act as recombination centers in $Al_{0.37}Ga_{0.53}As$ solar cells above ~70 K.[9] There are, however, limited data regarding dopant behavior in $Al_{0.23}Ga_{0.77}As$ grown by LPE.

(Received April 16, 2014; accepted July 19, 2014; published online August 14, 2014)

In this paper we report Hall effect studies on Sn, Te, Ge, Zn, Mg, and unintentionally doped $Al_xGa_{1-x}As$ (x = 0.23–0.24) grown by LPE. On the basis of the results we conclude that Mg has the same acceptor level as the p-type background dopant, and that DX centers are dominant in Sn doped samples but not in Te doped samples.

EXPERIMENTAL

All growth was conducted in a custom LPE system.[10] To summarize, the apparatus was designed as a rotating chamber, and primarily consisted of a graphite substrate holder and a graphite melt chamber. After surface treatment with aqueous ammonia solution for 3 min followed by DI water rinse to remove the native oxide, a semi-insulating GaAs (SI-GaAs) substrate (1 cm × 1 cm) was loaded into the system together with a melt consisting of 99.99999% pure Ga, 99.999% pure Al, polycrystalline GaAs saturation wafers in excess of the solubility limit, and the corresponding dopant. Ga was used as solvent. The Al-to-Ga weight ratio chosen was approximately 7.8×10^{-4}, to achieve the desired Al solidus composition. To start, the substrates were positioned next to the melt. The system was then purged with high-purity forming gas (4% H_2 in N_2), heated to 857°C, and held at that temperature for 2 h. Subsequently, the system temperature was reduced to 853°C to ensure the overall saturation of the melt. The growth commenced as we rotated the substrate into the melt and cooled the system to 850°C at 0.1°/min, which usually led to growth of a 5–6-μm epilayer. When the growth finished, the substrate was removed from the melt and the system was cooled to room temperature.

Growth of Sn-doped AlGaAs involved growth of an additional window layer of $Al_xGa_{1-x}As$ ($x \sim 0.9$) on top of the ~1.75 eV AlGaAs epilayer. The window layer was later etched away in concentrated HCl. This window layer was essential, because Sn-doped samples consistently have residual melt on them after growth, which leads to unwanted growth of rapid cooling layers and would have invalidated the Hall effect results. The rapid cooling layers were easily removed as the window layer below was etched away.

n-Type Hall contacts were formed by soldering 70:30% (w/w) In–Sn in the center of the sides of the square sample, on to the epilayer, then annealing at 450°C for 15 min. The p-type Hall contacts were formed by using 95:5% (w/w) In–Zn without annealing. Hall effect measurements were performed by use of an Ecopia HMS-5300 variable-temperature (80–350 K) Hall effect measurement system. Epilayer thickness was measured by use of cross-sectional scanning electron microscopy (SEM) with an FEI 430 NanoSEM. To verify the bandgap of AlGaAs, continuous-wave photoluminescence (cw-PL) was performed with a 552-nm diode laser with an output power of 20 mW (Coherent OBIS).

RESULTS AND DISCUSSION

All the samples in this work had bandgap energies of 1.76 ± 0.01 eV, with full width at half maximum (FWHM) ranges from 28 to 61 meV. Compared with the PL FWHM of ~35 meV obtained from low-pressure MOCVD-grown $Al_{0.2}Ga_{0.8}As$,[7] the compositional grading of AlGaAs because of the large distribution coefficient of Al in LPE is moderate. Three unintentionally doped samples were first grown to characterize the background doping concentration. Room temperature Hall measurements revealed p-type conductivity for all three samples, with carrier concentrations of 4.8×10^{16} cm^{-3}, 5.2×10^{16} cm^{-3}, and 3.7×10^{16} cm^{-3} and respective Hall mobility of 193 cm^2/V S, 181 cm^2/V S, and 202 cm^2/V S. The Hall mobility of AlGaAs in this work is usually better than the Hall mobility obtained from MBE-grown AlGaAs with a similar bandgap,[11] indicating that LPE-grown AlGaAs has a superior crystalline quality in terms of scattering. The average background doping concentration of 4.6×10^{16} cm^{-3} was used in subsequent analysis.

Figure 1a shows the relationship between carrier concentration and atomic fraction of different dopants in the melt at room temperature. From the figure, Te is an ideal n-type dopant for heavily doped AlGaAs, with the electron concentration varying almost linearly with Te atomic fraction in the melt when that fraction is less than 0.02%. Surface deterioration occurred when more Te was added into the melt, and the electron concentration was no longer sensitive to the amount of Te. In contrast, Sn is useful when lightly n-type doped AlGaAs is desired. The doping efficiency of Sn decreases as the electron concentration increases, mainly because of self-compensation.[12] Surface deterioration was also observed for Sn-doped samples when the atomic fraction of Sn exceeded 10%.

Hole concentration increases almost linearly with Zn fraction in the melt for Zn-doped AlGaAs at moderate doping levels. However, when the hole concentration exceeds 10^{18} cm^{-3}, the epilayer surface, again, deteriorates. For Ge-doped samples, exceptions to the linear relationship happen at low doping concentrations. Nelson and Robson attributed this to the relatively deep acceptor level of Ge.[13] Hall mobility at different carrier concentrations for four dopants is plotted in Fig. 1b as a reference for the quality of the material.

Results from temperature-dependent Hall measurements are shown in Fig. 2. Samples with carrier concentrations below 10^{18} cm^{-3} at room temperature were chosen, to avoid dopant saturation[14] and a significant band-narrowing effect at high dopant concentrations.[15,16] In fact, activation energies obtained from heavily Ge-doped GaAs samples ($N_A - N_D \approx 2 \times 10^{18}$ cm^{-3}) were shown to be invalid.[17] To derive the activation energies, the relationship

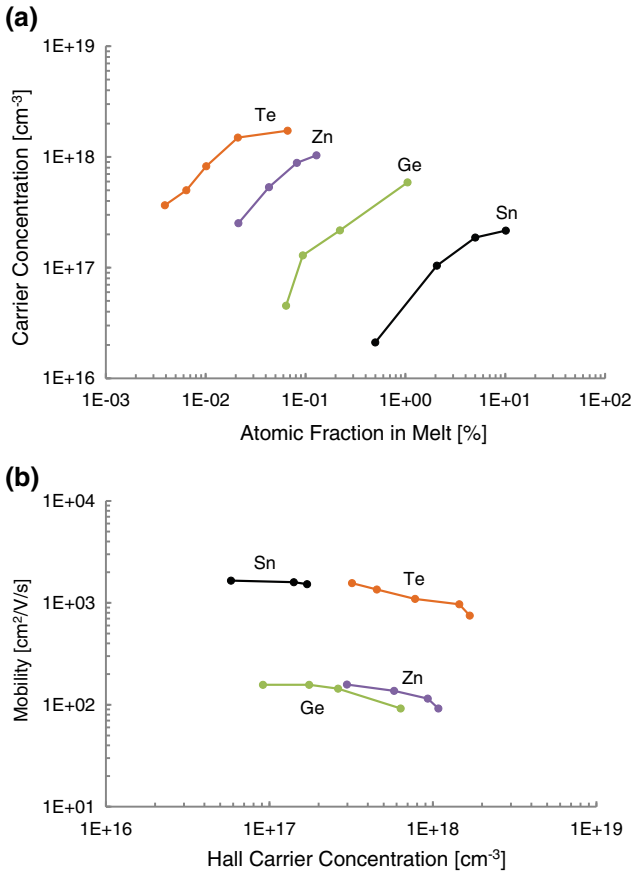

Fig. 1. (a) Carrier concentration as a function of atomic fraction for a variety of dopants in the melt at room temperature. The electron concentration was calculated by adding the average background doping concentration to the actual measured Hall electron concentration. The hole concentration was calculated by subtracting the average background doping concentration from the actual measured Hall hole concentration. (b) Hall mobility at different carrier concentrations. The Hall carrier concentration is the carrier concentration obtained directly from the Hall effect.

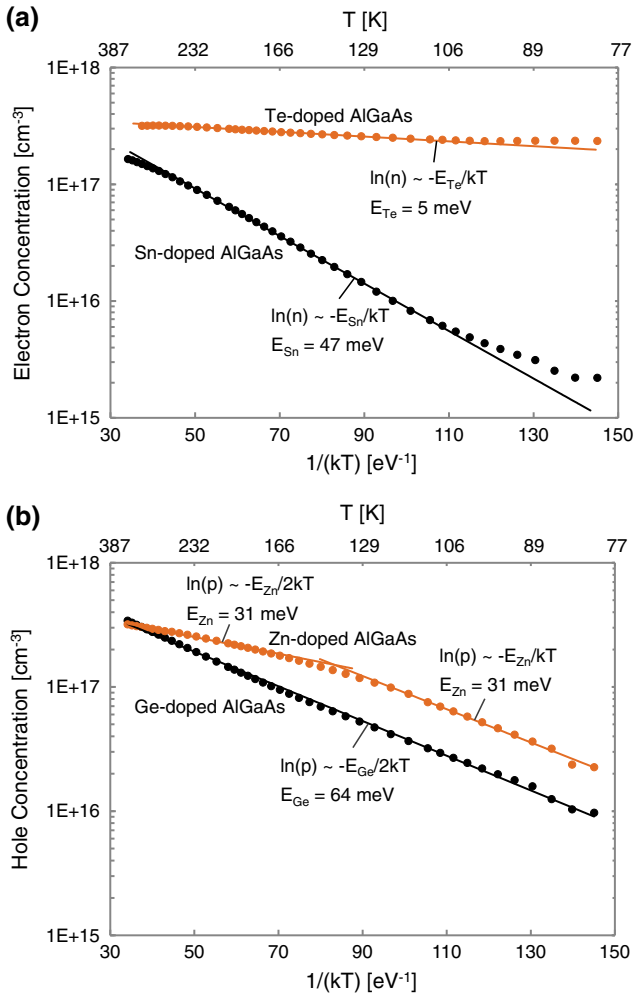

Fig. 2. Temperature-dependent Hall effect results for (a) Te and Sn-doped AlGaAs, where E_{Sn} and E_{Te} are the activation energies of Sn and Te, respectively, and (b) Zn and Ge-doped AlGaAs, where E_{Zn} and E_{Ge} are the activation energies of Zn and Ge, respectively. n and p are the electron and hole concentrations, respectively, k is the Boltzmann constant and T is the absolute temperature. Dots indicate measured data points and lines represent least-squares fits.

$$c \sim \exp\left(-\frac{E_A}{kT}\right), \tag{1}$$

was used when the material was compensated whereas when the compensation was negligible the relationship

$$c \sim \exp\left(-\frac{E_A}{2kT}\right) \tag{2}$$

was used.[18,19] In these equations, c is the carrier concentration, E_A is the activation energy of a specific dopant, k is the Boltzmann constant, and T is the temperature. For n-type AlGaAs doped at low 10^{17} cm^{-3}, it is plausible that the compensation in the epilayer cannot be ignored, considering the background p-type doping. Therefore, the relationship in Eq. 1 was used to fit both curves in Fig. 2a. For Sn-doped $Al_{0.24}Ga_{0.76}As$ samples, a relatively large activation energy of 47 meV was found, indicative of DX centers. It should be noted that a shallow donor level will still exist in the presence of DX centers,[18,19] corresponding to the data points at lower temperatures ($T < 100$ K) for which smaller slope is observed. For Te-doped $Al_{0.24}Ga_{0.76}As$ samples, an activation energy of 5 meV suggests that the shallow donor level is the dominant donor level in this material. The activation energy obtained for this shallow donor level also agrees with literature, in which a few meV are usually reported.[20]

For Ge-doped $Al_{0.24}Ga_{0.76}As$ samples, if we assume that the compensation from major donors is negligible and therefore use the relationship from Eq. 2 to fit the data points in Fig. 2b, we obtain an activation energy of 64 meV, which is in good agreement with predictions both from Hall data[21] and from low-temperature photoluminescence data.[22] Zn-doped $Al_{0.23}Ga_{0.77}As$ samples clearly give

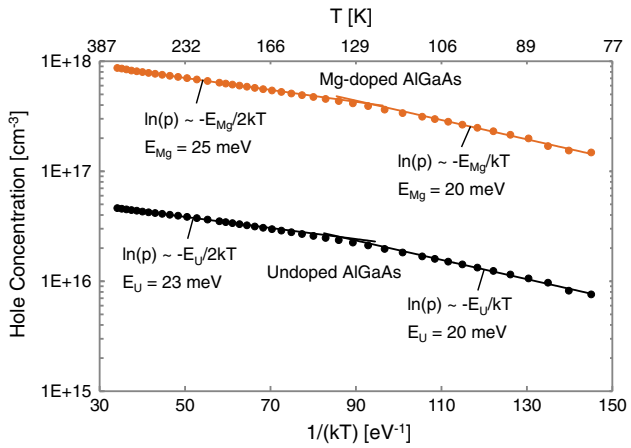

Fig. 3. Temperature-dependent Hall effect results for undoped and Mg-doped AlGaAs. E_{Mg} and E_U are the activation energies of Mg and the background dopant, respectively. p is the hole concentration, k is the Boltzmann constant and T is the absolute temperature. Dots indicate measured data points and lines represent least-square fits.

two different slopes in Fig. 2b. In addition, the linear fit at low temperatures has a slope that is twice that of the linear fit at higher temperature, leading us to believe that the material is partially compensated at low temperatures and the compensation becomes negligible as temperature increases. An activation energy of 31 meV was obtained by fitting Eq. 1 to the data in the low-temperature region, whereas fitting Eq. 2 to the data in the high-temperature region resulted in a similar value of 31 meV. The activation energies agree well with previous Hall studies predictions,[23] but are slightly smaller than the result from low-temperature photoluminescence, which yields an activation energy of ~40 meV.[22] Given that the assumption of negligible compensation from major donors worked well for Ge-doped samples within the whole temperature range, there must be other compensation mechanisms for the Zn-doped sample which caused compensation at low temperatures. The exact mechanism still needs further investigation.

By comparing temperature-dependent Hall effect results for undoped samples and Ge or Zn doped samples, we found that the activation energy of the background dopant was smaller than that of either Ge and Zn. Therefore, an Mg-doped $Al_{0.24}Ga_{0.76}As$ sample was grown; it had the same acceptor activation energy as the undoped $Al_{0.24}Ga_{0.76}As$ sample, as shown in Fig. 3. Therefore, either the background dopant is Mg or it induces the same defect level as for the Mg-doped sample. The exact cause requires further investigation. Baking the system at 900°C first with graphite parts exposed to high-purity forming gas for 12 h, then baking again at 900°C with all the melt chambers filled with 2:98% (w/w) Al–Ga under high purity forming gas for 12 h did not reduce the background concentration. The activation energy of 20 meV for Mg obtained by fitting Eq. 1 to low-temperature data points is consistent with previous Hall studies predictions.[14] A slightly larger activation energy was obtained by fitting Eq. 2 to high-temperature data, indicating low levels of compensation at high temperatures.

In summary, we performed Hall effect studies on undoped and Sn, Te, Ge, Zn, and Mg-doped $Al_xGa_{1-x}As$ (x = 0.23–0.24) grown by LPE. The study is essential for optimizing $Al_{0.23}Ga_{0.77}As$ solar cells, a suitable top sub-cell on Si, especially via wafer bonding and subsequent epitaxial lift-off. Our study suggests Te is a suitable dopant for n-type emitters in solar cells, because of its low activation energy and efficient doping capacity below 1.5×10^{18} cm^{-3}. An undoped base can be used, because we eliminated the possibility that deep acceptors contributed to the background doping, and increased hole concentration can be realized by introducing Ge into the material.

REFERENCES

1. T.P. White, N.N. Lal, and K.R. Catchpole, *IEEE J. Photovolt.* 4, 208 (2014).
2. S.R. Kurtz, P. Faine, and J.M. Olson, *J. Appl. Phys.* 68, 1890 (1990).
3. J.R. Lang, J. Faucher, S. Tomasulo, K.N. Yaung, and M.L. Lee, *Appl. Phys. Lett.* 103, 092102 (2013).
4. I. Vurgaftman, J.R. Meyer, and L.R. Ram-Mohan, *J. Appl. Phys.* 89, 5815 (2001).
5. K. Tanabe, K. Watanabe, and Y. Arakawa, *Sci. Rep.* 2, 1 (2012).
6. J.M. Woodall, R.M. Potemski, S.E. Blum, and R. Lynch, *Appl. Phys. Lett.* 20, 375 (1972).
7. M.R. Islam, R.V. Chelakara, J.G. Neff, K.G. Fertitta, P.A. Grudowski, A.L. Holmes, F.J. Ciuba, R.D. Dupuis, and J.E. Fouquet, *J. Electron. Mater.* 24, 787 (1995).
8. E.F. Schubert, *Light-Emitting Diodes* (Cambridge: Cambridge University Press, 2003), pp. 1–7.
9. S. Heckelmann, D. Lackner, F. Dimroth, and A.W. Bett, *Appl. Phys. Lett.* 103, 132102 (2013).
10. X. Zhao, K.H. Montgomery, and J.M. Woodall, *J. Electron. Mater.* 43, 894 (2014).
11. W.C. Liu, *J. Mater. Sci.* 25, 1765 (1990).
12. M.B. Panish, *J. Appl. Phys.* 44, 2667 (1973).
13. A.W. Nelson and P.N. Robson, *J. Appl. Phys.* 54, 3965 (1983).
14. S. Mukai, Y. Makita, and S. Gonda, *J. Appl. Phys.* 50, 1304 (1979).
15. M.K. Hudait, P. Modak, S. Hardikar, and S.B. Krupanidhi, *J. Appl. Phys.* 82, 4931 (1997).
16. S.C. Jain, J.M. McGregor, and D.J. Roulston, *J. Appl. Phys.* 68, 3747 (1990).
17. G.B. Stringfellow and R. Linneback, *J. Appl. Phys.* 51, 2212 (1980).
18. E.F. Schubert and K. Ploog, *Phys. Rev. B* 30, 7021 (1984).
19. P.M. Mooney, *J. Appl. Phys.* 67, R1 (1990).
20. N. Chand, T. Henderson, J. Clem, W.T. Masselink, R. Fischer, Y.C. Chang, and H. Marko, *Phys. Rev. B* 30, 4481 (1984).
21. A.J. Springthorpe, F.D. King, and A. Becke, *J. Electron. Mater.* 4, 101 (1975).
22. R. Hellman and G. Oelgart, *Semicond. Sci. Technol.* 5, 1040 (1990).
23. K. Masu, M. Konagai, and K. Takahashi, *J. Appl. Phys.* 51, 1060 (1980).